framatome

SUNSI Review Complete
Template = ADM-013
E-RIDS=ADM-03
ADD: Jazel Parks, Edward O'Donnell

COMMENT (19)
PUBLICATION DATE: 7/30/2019
CITATION 84 FR 36961

November 13, 2019
NRC:19:029

Office of Administration
ATTN: Program Management, Announcements and Editing Staff
Mail Stop: TWFN–7–A60M
U.S. Nuclear Regulatory Commission
Washington, DC 20555–0001

Framatome Inc. Response to Request for Public Comment on the Draft Regulatory Guide DG-1327, "Pressurized Water Reactor Control Rod Ejection and Boiling Water Reactor Control Rod Drop Accidents" (Federal Register Vol. 84, No. 146, 36961, dated July 30, 2019; Docket ID NRC-2016-0233)

Ref. 1: Federal Register Vol. 84, No. 146, 36961, dated July 30, 2019; Docket ID NRC-2016-0233.

Ref. 2: Draft Regulatory Guide DG-1327, "Pressurized Water Reactor Control Rod Ejection and Boiling Water Reactor Control Rod Drop Accidents," July 2019 (ML18302A106).

Ref. 3: Federal Register Vol. 84, No. 181, 49125, dated September 18, 2019; Docket ID NRC-2016-0233.

Dear Rulemaking and Adjudications Staff:

Framatome Inc. (Framatome) submits the enclosed comments for consideration by the U.S. Nuclear Regulatory Commission (NRC). These comments are in response to the NRC request for public comment on the Draft Regulatory Guide DG-1327, "Pressurized Water Reactor Control Rod Ejection and Boiling Water Reactor Control Rod Drop Accidents" (Federal Register Vol. 84, No. 146, 36961, dated July 30, 2019; Docket ID NRC-2016-0233 (Reference 1 and 2)). The comment period was extended to November 18, 2019 in Reference 3.

Framatome also participated with the Regulatory Technical Advisory Committee (Reg TAC) of the EPRI Fuel Reliability Program in developing the Industry responses to the Draft Regulatory Guide DG-1327 that NEI will be submitting to the NRC. Framatome is in general concurrence with the Industry comments contained in the NEI submittal except as clarified by the enclosed Framatome specific comments on the draft rule language.

Framatome Inc.
3315 Old Forest Road
Lynchburg, VA 24501
Tel: (434) 832-3000

www.framatome.com

There are no new commitments within this letter or its enclosures.

If you have any questions related to this information, please contact Mr. Alan Meginnis by telephone at (509) 375-8266, or by e-mail at Alan.Meginnis@framatome.com

Sincerely,

Gary Peters, Director
Licensing & Regulatory Affairs
Framatome Inc.

cc: J. G. Rowley
Project 728

Enclosures

1. Framatome Comments on DG-1327

Enclosure 1:
Framatome Comments on DG-1327

Comment #1: DG-1327, page 6, 1st paragraph.

Statement in Guidance: "The prompt thermal expansion of the fuel pellet, which can be exacerbated at high burnups by gaseous fission product swelling, may cause the fuel cladding to fail by PCMI, which is enhanced by the presence of hydrogen in the cladding."

Description of Concern: The last phrase can be misinterpreted to suggest that hydrogen enhances PCMI. The impact of hydrogen is on the potential for cladding failure.

Basis for concern: Clarity.

Proposal: "The prompt thermal expansion of the fuel pellet, which can be exacerbated at high burnups by gaseous fission product swelling, may cause the fuel cladding to fail by PCMI. The potential for failure is enhanced by the presence of hydrogen in the cladding."

Basis for proposal: Clarity.

References: None

Comment #2: DG 1327, Section 1.2.3 (p. 7)

Statement in Guidance: "Because of the dominant role liner fuel test results played in the development of the RXA PCMI cladding failure threshold curves and the influence of the sponge or low-alloy zirconium liner on the initial hydride distribution, the applicability of these failure threshold curves for nonliner cladding designs is limited to cladding with less than 70 weight parts per million (wppm) excess hydrogen."

Description of Concern: A limit of 70 wppm of excess hydrogen creates undue burden for M5 cladding material.

Basis for concern: Technical justification for the 70 wppm limit and the assessment of burden for each cladding material is provided on pp. 25-26 of Reference 1. In that discussion, it is noted that M5 is "unlikely to absorbed more than 100 wppm of hydrogen at end of life." This presumption appears to be based on measured data from typical M5 cladding fuel rods; however, it is not an accurate reflection of the upper bound predictions of cladding hydrogen content that would typically be used in the safety analysis of RIA type events. The assessment in Reference 1 also used a solubility limit of 75 wppm for PWR operating conditions which is too high for typical hot zero power (HZP) coolant conditions. HZP coolant temperatures are approximately 550°F and the hydrogen solubility limit is in the range of 50-55 wppm. Based on these observations, the limit of 70 wppm for non-liner RXA cladding does create undue burden for M5 cladding.

Proposal: Based on the arguments presented, delete Section 1.2.3 from DG-1327.

Basis of proposal:

Framatome does not believe that the influence of the sponge or low-alloy zirconium liner on the initial hydride distribution invalidates the use of RXA PCMI cladding failure threshold curves. The bases for this position are as follows.

1. The PCMI failure mechanism during the initial stage of the RIA transient was identified to be the "outside-in" hydride-assisted cracking, for both SRA and RXA cladding types. As shown in Figure 1 below, taken from Reference 2, the crack initiation occurs at the cladding outer surface, where either a dense hydride rim (PWR, SRA cladding), or a highly connected hydride network with strong radial component (BWR, RXA cladding) develops with increasing exposure; the final crack propagation through the inner half region of the cladding is very fast, as it occurs under increasing stress intensification at the tip of the propagating crack.
2. It is generally acknowledged that RXA zirconium alloys have higher propensity for radial hydrides and thus they become more brittle at lower hydrogen concentrations than SRA material, which requires the development of a sufficiently thick outer hydride rim for crack initiation to occur – this PWR hydride rim is equivalent to the radial hydride network in RXA material.
3. The overall cladding ductility has a negligible impact on the hydride-assisted outside-in cracking mechanism in the initial PCMI phase of RIA transients – this was documented in the PIE for the NSRR tests, which show typical final ductile failure due to the stress

intensification at the tip of the crack exceeding the ultimate tensile strength (UTS) (illustration in Figure 2)

4. During normal operation and cool downs, the less alloyed liner at the cladding inner surface soaks up some of the hydrogen from the inner half of the cladding, but the outer hydride structure is not significantly affected – this is because the hydrogen diffusion is directed down the temperature gradient and thus quickly balances the concentration gradient created by the liner in the opposite direction– this is illustrated by Figure 3 from Reference 4, which shows that the hydrogen in the liner migrates down the temperature gradient during the power ramp over a small region next to the liner, which was also the region that supplied hydrogen to the liner during reactor operation.
5. In Reference 1 (pp. 25 and 26), Reference 2 was used to argue that the liner soaking effect renders the liner cladding more ductile overall than a non-liner cladding with the same total H content – this characterization is however dependent on the loading condition during the RIA transient and the type of mechanical tests used to investigate cladding behavior. The studies reported in Reference 2 used Ring Compression Tests (RCT), which were performed on cladding that experienced Hydride Reorientation Treatment (HRT); therefore, the cladding condition is not representative of as-irradiated cladding and the loading during an RCT is very different from the loading (uniform tensile strain) during the PCMI-RIA phase.
6. The RCT is a bending test that creates a large stress gradient across the cladding thickness: tensile and compressive stresses at the inner and outer surfaces, respectively at the point where the compressive load is applied and the opposite stress gradient at 90° from that point. Initially, the inner surface tensile stress is higher at the point of compressive load, but afterwards the tensile stress at the outer surface at the 90° position becomes larger. Because of the radially re-oriented hydrides in the non-liner HRT samples reported in Reference 2, the crack was initiated at clad inner surface. The liner HRT samples cracked later from the outer surface, because of the migration of hydrogen from the outer half of the liner region during the HRT (see metallography samples in Reference 2).
7. While the liner cladding has an apparent higher ductility in case of the RCT, this cannot be extended to the different loading and hydride morphology condition of as-irradiated cladding during a RIA-PCMI test.
8. The amount of hydrogen near the exterior of the cladding is the important quantity that is related to failure enthalpy. Using the total hydrogen (for plotting against failure enthalpy) is a reasonable simplification relative to estimating the amount of hydrogen in the exterior portion of the cladding.
9. In addition, Framatome proprietary Expansion Due to Compression (EDC) tests performed in a hot cell on irradiated cladding samples, showed similar behavior of liner and non-liner samples. The EDC test simulates the loading condition during RIA-PCMI to a large extent, although the stress ratio is somewhat different. Nevertheless, the cladding hydride morphology was representative and given the similar loading state, the EDC results support the conclusion of a negligible impact of the liner hydrogen soaking effect for RIA-PCMI.

Alternative Proposal: If the proposal above is not considered an acceptable proposal, then revise Section 1.2.3 to provide adjusted PCMI limits for non-liner RXA cladding.

PCMI limit curves for non-liner RXA cladding materials can be developed by adjusting the hydrogen content of the liner RXA cladding tests to account for the influence of the liner on the hydrogen distribution in the bulk cladding material. Examples of adjusted PCMI limit curves are provided below in Figures 4 and 5.

Basis of alternative proposal:

Hydrogen distribution through the cladding wall has been measured by Hayashi et al (References 3 and 4) and also in the NFIR-V project (References 5 and 6). Figure 6 shown below is taken from Reference 2 and demonstrates the preferential accumulation of hydrogen in the liner at the interface with the bulk cladding. These distributions (References 3 through 6) were used to evaluate the reduction in the bulk metal hydrogen concentration due to the soaking effect of the liner. On average, the soaking effect of the liner reduces the bulk hydrogen content by ~21% compared to the total hydrogen value. The upper bound is < 30% reduction. Figure 7 shows the results of the evaluation.

These results were also used to evaluate the hydrogen distribution in more than 30 Framatome proprietary metallographic cross-sections of lined Zr-2 RXA cladding from multiple BWR plants. The evaluation concluded that an upper bound reduction factor of 30% is conservative for total hydrogen content in excess of 800 wppm.

The RIA test data also provides evidence that the reduction can be no larger than ~30%. For example test Fk-9 (failed) with excess hydrogen of ~150 wppm would be adjusted to 105 wppm using a 30% reduction factor. Reductions larger than this would push this data point into the population of non-failed tests that include both liner and non-liner cladding. Consequently, reductions larger than 30% are not realistic.

Revised PCMI limit curves for non-liner RXA cladding can be developed by reducing the excess hydrogen content for the group of failed tests in the range of 150-200 wppm (see Reference 1, p. 47). Using this technique, PCMI limit curves are provided below in Figures 4 and 5. After the shift, the data points do not align well with a power function as proposed in Reference 1, p. 47. While more exotic function combinations could be used to fit the data, a simple, piecewise linear fit is provided in Figures 4 and 5.

References:

1. Response to Public Comments – Draft Regulatory Guide (DG)-1327, "Pressurized Water Reactor Control Rod Ejection and Boiling Water Reactor Control Rod Drop Accidents," Proposed New Regulatory Guide, July 2019. (ML18302A107)
2. M. Aomi, T. Baba, T. Miyashita, K. Kamimura, T. Yasuda, Y. Shinohara, and T. Takeda, "Evaluation of Hydride Reorientation Behavior and Mechanical Properties for High-Burnup Fuel-Cladding Tubes in Interim Dry Storage," Journal of ASTM International, Vol.5, No. 9, 2011.
3. H. Hayashi, et al., "Outside-in Failure of High Burnup BWR Segment Rods Caused by Power Ramp Tests", Proceedings 2003 International Topical Meeting. on LWR Fuel Performance, Würzburg, Germany, (2003).
4. S. Shimada, et al., "A Metallographic and Fractographic Study of Outside-In Cracking Caused by Power Ramp Tests," Journal of Nuclear Materials 327 (2004), 97.
5. NFIR-V/EPRI, "The NFIR-V Cladding Project - Hydride Reorientation Studies (Topic 5)," "CEA Saclay – 8th Semi-Annual Report," X105-05-CEA-08, October 2009.
6. Q. Auzoux, et al., "Hydride Reorientation and its Impact on Ambient Temperature Mechanical Properties of High Burn-Up Irradiated and Unirradiated Recrystallized Zircaloy-2 Nuclear Fuel Cladding with an Inner Liner," Journal of Nuclear Materials 494 (2017), 114.

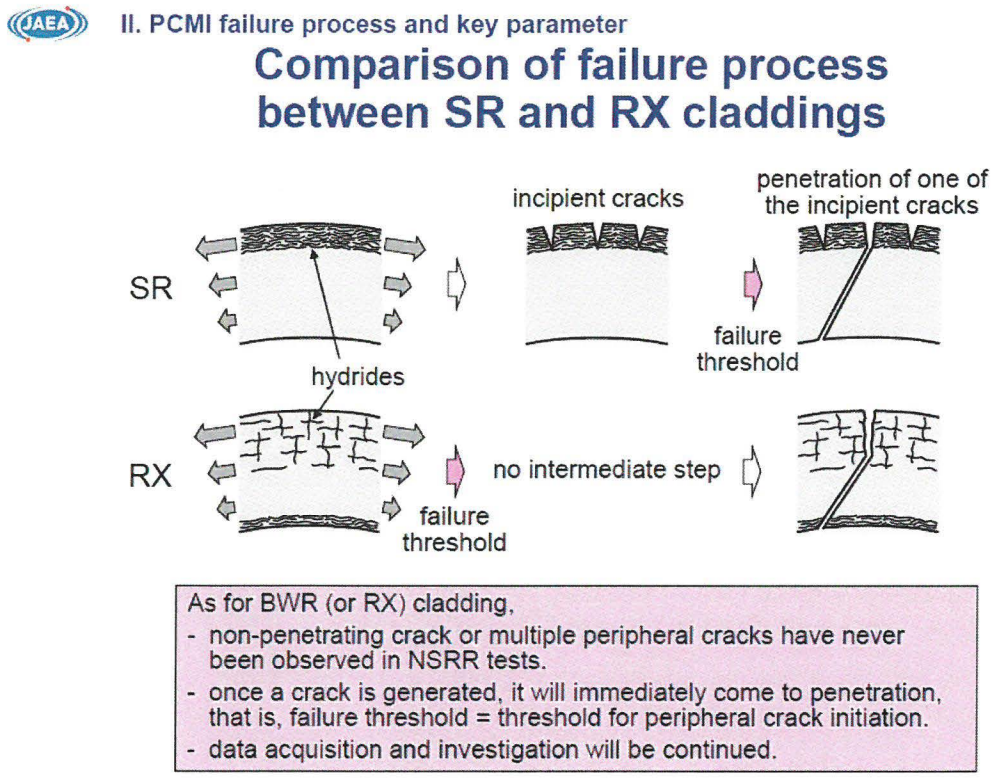

Figure 1: Hydride-assisted PCMI-RIA failure mode from presentation of Reference 2

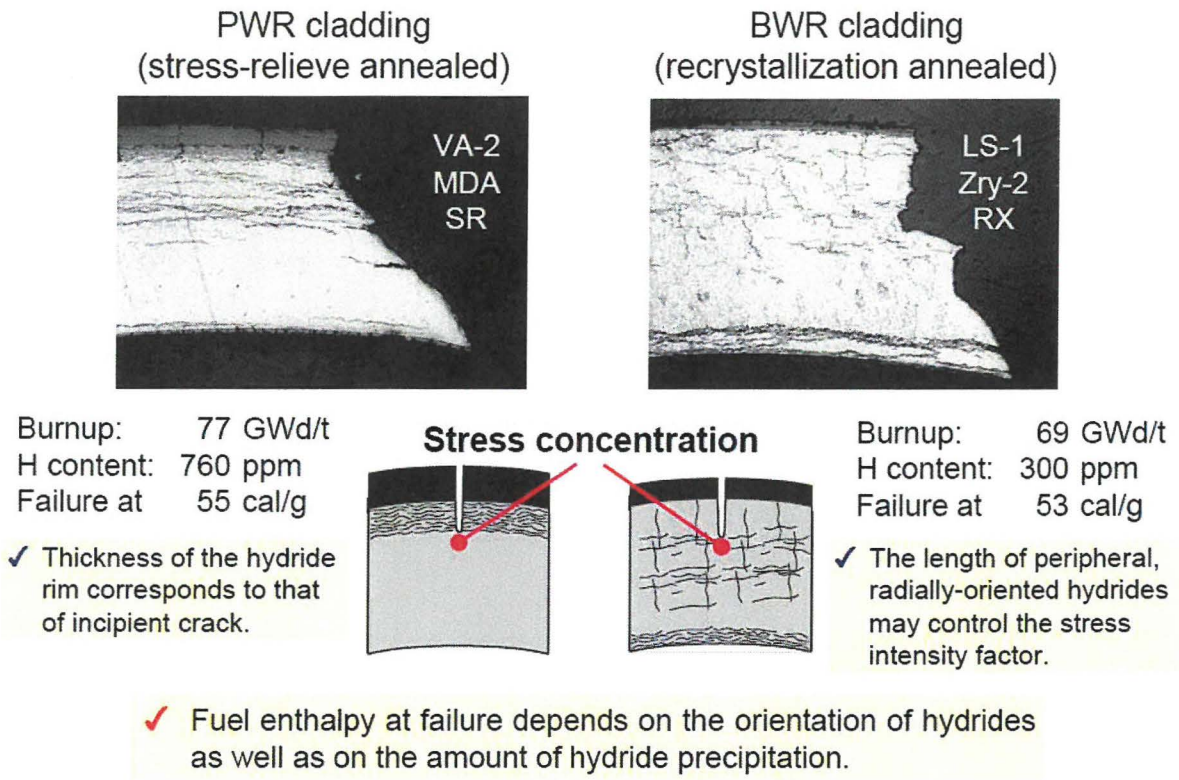

Figure 2: Similar hydride-assisted PCMI-RIA failure mode for PWR (CWSR) and BWR (RXA) cladding types

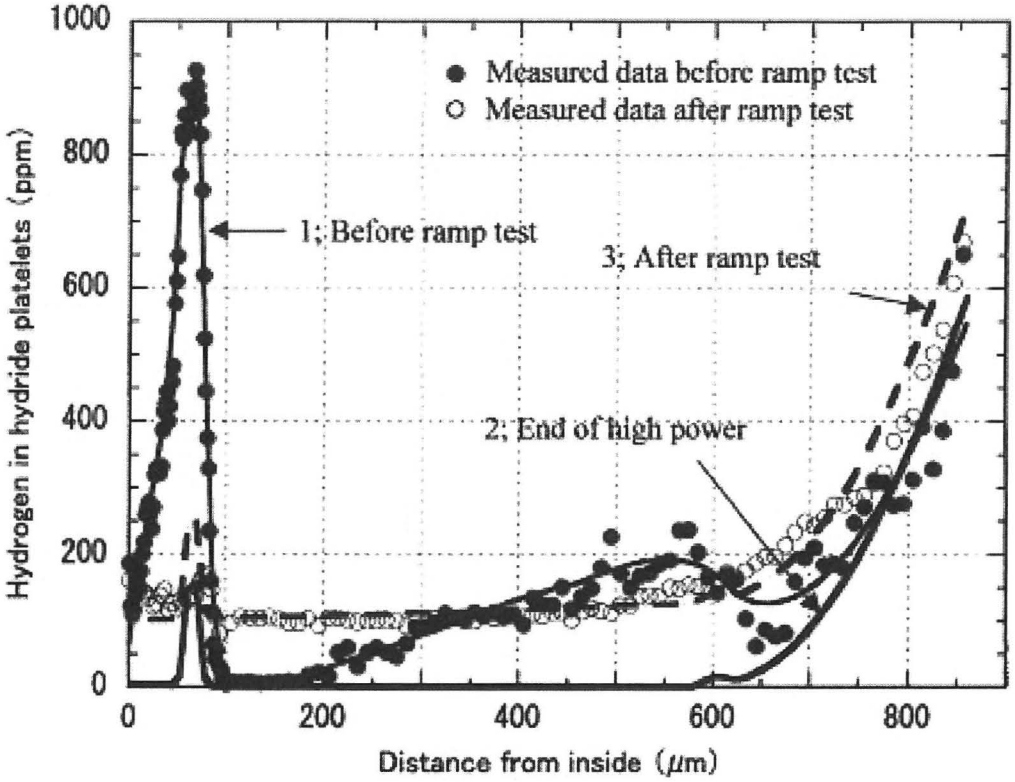

Figure 3: Hydride distribution before and after a power ramp, showing small region next to the liner that is affected by liner soaking effect

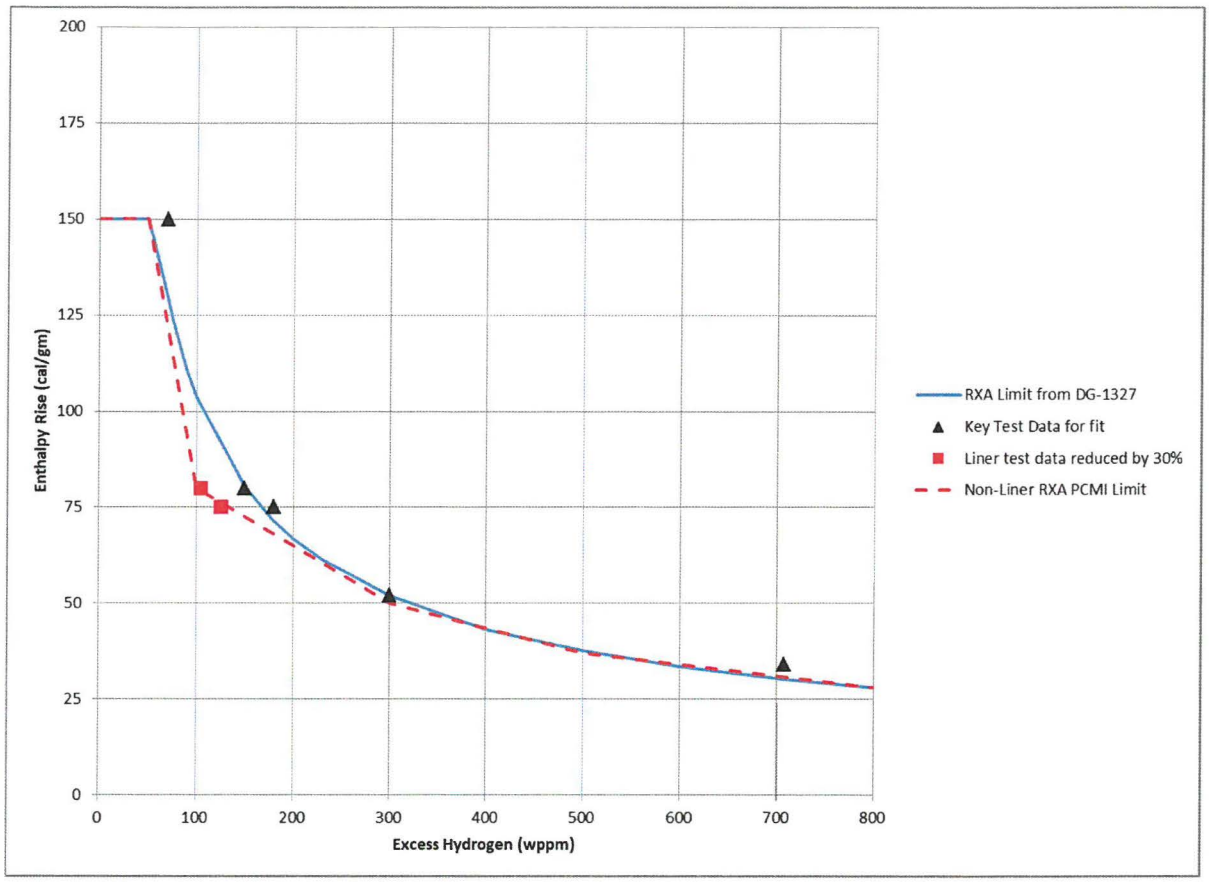

Figure 4: Example PCMI Cladding Failure Threshold – Non-Liner RXA Cladding below 500 Degrees F

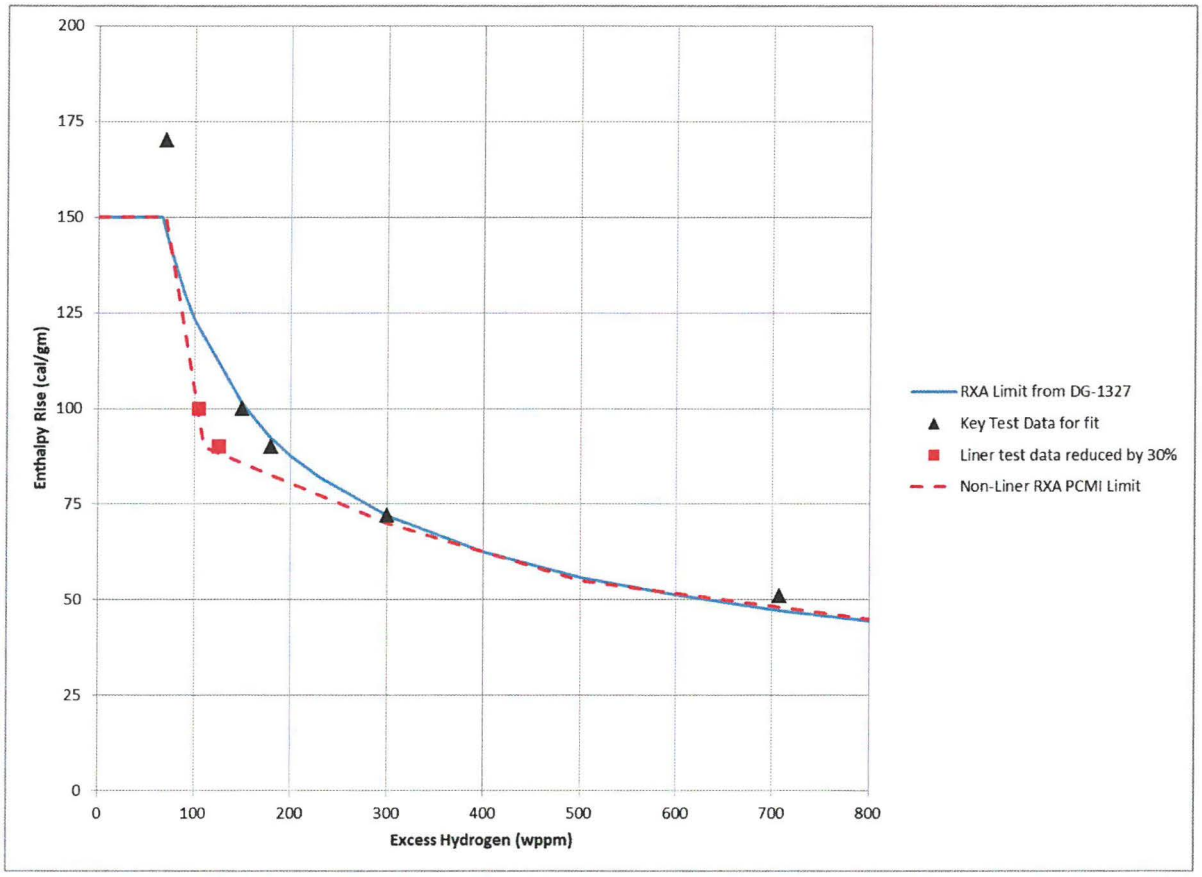

Figure 5: Example PCMI Cladding Failure Threshold – Non-Liner RXA Cladding above 500 Degrees F

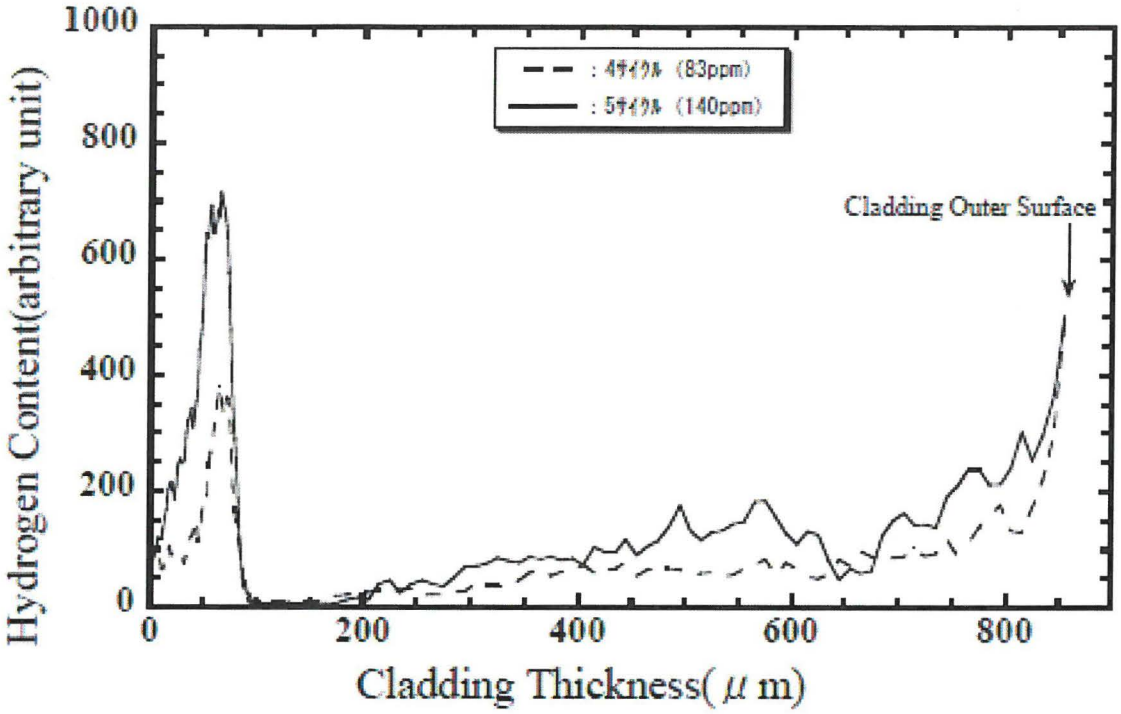

Figure 6: Hydrogen Distribution from Hayashi et el (Reference 2)

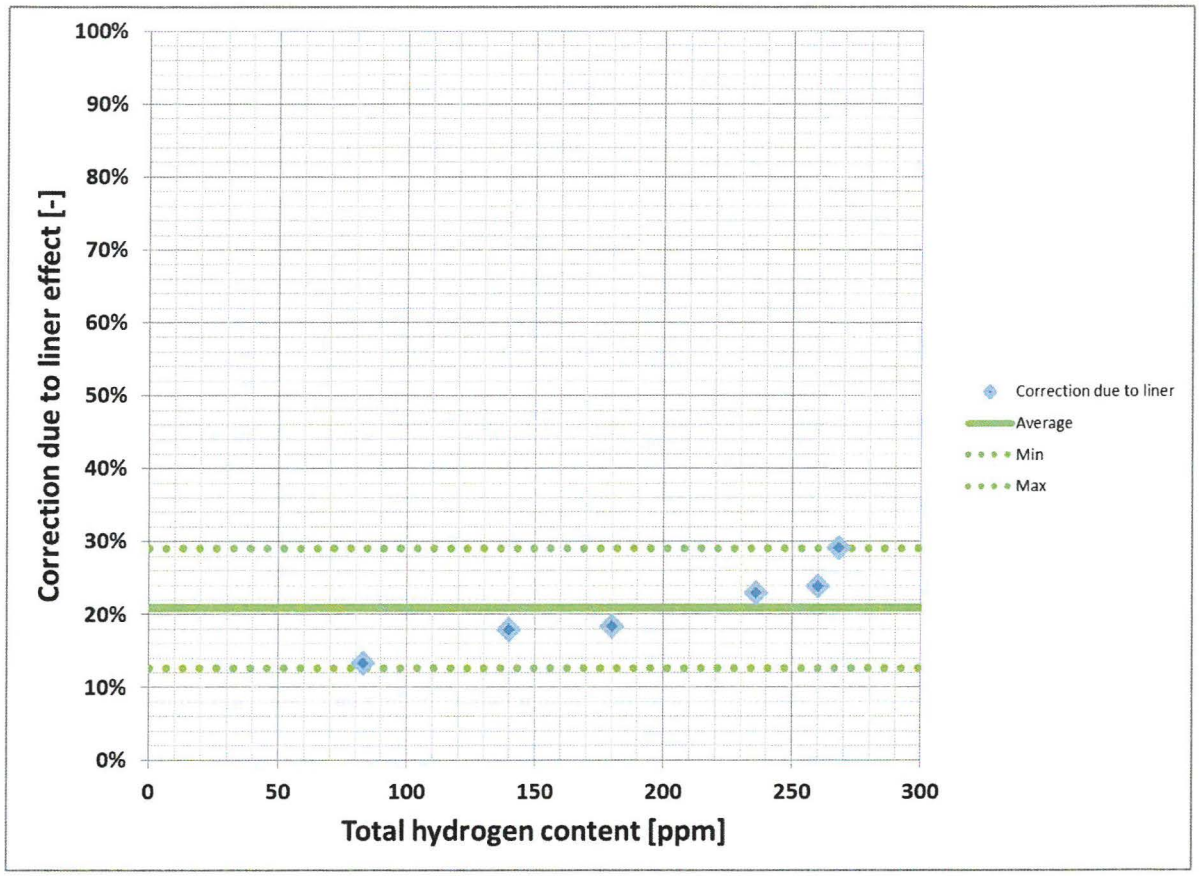

Figure 7: Hydrogen Concentration Reduction due to Linear Soaking Effect

Comment #3: DG-1327, Section 2.3.5 (p. 13)

Statement in Guidance: "Each applicant should address the possibility of hydride reorientation because of power maneuvering or reactor shutdown."

Description of Concern: The statement in the guidance is vague and does not agree with the public comment resolution stated in Reference 1, p. 29.

Basis for concern: Without specific guidance this item is subject to misinterpretation. The current statement is not in agreement with the public comment resolution in Reference 1, pp. 28-29.

Proposal: Consider the following revision:

"Each applicant should address the possibility of hydride reorientation because of power maneuvering or reactor shutdown consistent with the requirements in NUREG 0800 Section 4.2 II. ACCEPTANCE CRITERIA, SRP Acceptance Criteria, 1.A. Fuel System Damage: vi (2), page 4.2-7, Revision 3, March 2007."

Basis for proposal: Direct reference to NUREG 0800 Section 4.2 provides unambiguous guidance for this item and agrees with the public comment resolution provided in Reference 1, p. 29.

References:

1. Response to Public Comments – Draft Regulatory Guide (DG)-1327, "Pressurized Water Reactor Control Rod Ejection and Boiling Water Reactor Control Rod Drop Accidents," Proposed New Regulatory Guide, July 2019. (ML18302A107).

Comment #4: DG 1327, Section 3.1 (pp. 14-15).

Statement in Guidance:

"3.1 High-Temperature Cladding Failure Threshold

Figure 1 shows the empirically based high-temperature cladding failure threshold. This composite failure threshold encompasses both brittle and ductile failure modes and should be applied for events initiated from reactor startup conditions up to 5-percent reactor power operating conditions. Because ductile failure depends on cladding temperature and differential pressure (i.e., rod internal pressure minus reactor pressure), the composite failure threshold is expressed in peak radial average fuel enthalpy (calories per gram (cal/g)) versus fuel cladding differential pressure (megapascals (MPa)).

For at-power operating conditions (i.e., above 5-percent reactor power), fuel cladding failure is presumed if local heat flux exceeds thermal design limits (e.g., departure from nucleate boiling and critical power ratios)."

Also, from Reference 1, p. 34:

> "c) The NRC disagrees with this comment. The proposed text does not cover a scenario involving a nonprompt power excursion initiated from below 5% power. For these events where the initial heat flux is extremely low, use of the at-power thermal design limits becomes questionable. Application of Figure 1 is appropriate for these cases, and the calculated fuel enthalpy will reflect the actual power excursion (prompt or non-prompt)."

Description of Concern: The RIA criteria for High-Temperature Cladding Failure Threshold are derived from RIA testing of fuel pins undergoing prompt critical power excursions. These power pulses have pulse widths < 0.05 seconds. The initial power level does not define whether there is a power pulse that needs to be evaluated against these criteria. The RAI criterion for High-Temperature Cladding Failure Threshold in the DG 1327 Figure 1 is not applicable to conditions where there is no power pulse.

The NRC approved Framatome topical report ANP-10338P-A (December 2017) reflects this by applying this criteria only to prompt critical pulses. DNBR is evaluated for non-prompt power pulses.

Basis for concern: The statement from Reference 1, p. 34 "For these events where the initial heat flux is extremely low, use of the at-power thermal design limits becomes questionable." is true for prompt critical excursions but is not true for non-prompt critical excursions from extremely low powers. Starting at extremely low powers with a non-prompt reactivity insertion does not result in a power pulse. A non-prompt reactivity insertion results in a prompt jump proportional to the original flux with a subsequent period of seconds rather than milliseconds and may not have a distinct pulse shape. For example, a reactivity insertion of 0.95$ would cause the flux to jump by a factor of 20 with a Period of ~1 sec. An initial power of 0.00001% power would jump to 0.00020% power and increase with a period of ~1 second. The power would slowly approach sensible heat and reach an asymptotic power as the feedback balances the reactivity insertion. Some overshoot in the neutron power may occur resulting in a very broad power response. The DNBR and fuel centerline melt (FCM) criteria are adequate to assess the integrity of the fuel for this type of event. This type of power excursion can be very similar to other HZP events that use the DNBR and FCM fuel failure criteria. The RIA specific criteria are based on testing with prompt critical reactivity excursions resulting in relatively

narrow pulse widths (<<0.1sec) which is not characteristic of non-prompt critical excursions from low powers. In addition, the enthalpy rise failure criterion defines the enthalpy rise as the enthalpy change from the start of the event to one pulse width after the power peak. For a non-prompt condition, enthalpy rise is not defined when the power asymptotically approaches a peak power and has no pulse width.

A prompt critical rod ejection case at 10 or 20% power that has a significant power pulse is appropriate to evaluate with the High-Temperature Cladding Failure Threshold during the pulse (versus using a DNBR criterion). After the pulse when the heat flux and neutron power reach relatively constant values, DNBR does become a valid criterion.

Proposal: The following wording is proposed.

3.1 High-Temperature Cladding Failure Threshold

Figure 1 shows the empirically based high-temperature cladding failure threshold. This composite failure threshold encompasses both brittle and ductile failure modes and should be applied for events with prompt critical excursions (i.e. the ejected rod worth or drop rod worth >1.0$). Because ductile failure depends on cladding temperature and differential pressure (i.e., rod internal pressure minus reactor pressure), the composite failure threshold is expressed in peak radial average fuel enthalpy (calories per gram (cal/g)) versus fuel cladding differential pressure (megapascals (MPa)). If the event reaches a significant power after the pulse where the heat flux and neutron power remain relatively constant, fuel cladding failure is presumed if local heat flux exceeds thermal design limits (e.g., departure from nucleate boiling and critical power ratios).

For non-prompt critical excursions, fuel cladding failure is presumed if local heat flux exceeds thermal design limits (e.g., departure from nucleate boiling and critical power ratios).

Basis of proposal: The revised wording results in the application of each criterion to the appropriate conditions. The non-prompt conditions at low power levels are easily shown to be less limiting than higher powered cases with existing SAFDLs. This approach is also applicable for a BWR in that the non-prompt cases at low power would be bound by the prompt cases at low power.

References:

1. Response to Public Comments – Draft Regulatory Guide (DG)-1327, "Pressurized Water Reactor Control Rod Ejection and Boiling Water Reactor Control Rod Drop Accidents," Proposed New Regulatory Guide, July 2019. (ML18302A107).

Comment #5: DG-1327, Section 6 (p. 18)

Statement in Guidance: "If fuel centerline melting occurs, the peak fuel temperature in the outer 90 percent of the fuel volume should remain below incipient fuel melting conditions."

Description of Concern: The term "centerline" is ambiguous for annular pellets. The text does not agree with the public comment resolution from Reference 1, p. 44.

Basis for concern: Use of the term "centerline" creates potential confusion for application to annular fuel pellets. This word could be deleted with no change to the intended meaning.

Proposal: Consider the following revision:

"If fuel melting occurs, the peak fuel temperature in the outer 90 percent of the fuel volume should remain below incipient fuel melting conditions."

Basis for proposal: Provides clarity for application to all fuel pellet types, including annular pellets. It also aligns with the public comment resolution provided in Reference 1, p. 44.

References:

1. Response to Public Comments – Draft Regulatory Guide (DG)-1327, "Pressurized Water Reactor Control Rod Ejection and Boiling Water Reactor Control Rod Drop Accidents," Proposed New Regulatory Guide, July 2019. (ML18302A107).

Comment #6: Appendix B, Table B-1, Footnote B1.

Statement in Guidance: "The fraction of Cesium in the gap provided in Table B-1 assumes a diffusion coefficient from the fuel to the gap that is 2 times the coefficient for Krypton (Kr)-85. "

Description of Concern: The Cesium fission gas release (FGR) is considered to be over-conservative.

Basis for concern:
As indicated by Sandia National Laboratory in Reference 1, the factor of 4 increase in the fission gap release fraction for alkali metals from 0.12 in Regulatory Guide 1.183 Rev. 0 to a value of 0.49 in the current guidance seems excessive. FRAPCON does not calculate Cesium's release / birth ratio (R/B). Rather, it is estimated by adjusting the Kr-85 gap release. The Sandia paper (Reference 1) indicates that this results in the FGR fraction for Cesium being very high relative to the other nuclide groups and measurements. The Cesium FGR is considered to be over conservative based on two mechanisms that inhibit the release to the gap: (1) holdup on the grain boundaries due to fuel matrix interaction with UO_2 compounds and (2) potential for Cesium that migrates from the grain boundaries to the gap to interact with the internal layer of Zirconium cladding. Although noble gas release clearly increases with burnup, this is not necessarily the case with Cesium. Analyses by Powers (2013) (Reference 2**)** concluded that the diffusion rate of Cesium species would be less than that of Xenon.

Proposal: Modify the Cesium FGR fraction to be based on Xenon rather than Krypton to better reflect experimental data. This modification would change Table B-1 and footnote B1 on p. B-1, Section B.2 on p. B-3, Section B-1.2 on pp. B-4 and B-5, and the example calculation on p. B-9.

Basis for proposal: References 1, 2, 3 and 4 indicate a direct relationship between Cs and Xe release as shown by the data in the table below, which was taken from Table 3 of Reference 3.

TABLE 3. Cs AND Xe RELEASE AT HIGH BURNUP [42]

PELLET BURNUP (GW·d/t U)	Cs RELEASE (%)	ROD BURNUP (GW·d/t U)	Xe RELEASE (%)*
102	26.3	98	26.0
90	19.9	90	19.0
83	11.0	78	12.5
67	8.2	63	9.0
65	8.0	60	8.2
50	8.0	45	7.0

* The release values for Xe are taken from the curve in Fig.18.

References:

1. "Release Fractions in Non-LOCA Accidents in Draft Regulatory Guide 1.183 DG-1199, Sandia Laboratory," N.C. Andrews & R.O. Gauntt (Accession No. ML19094A336.pdf).
2. Powers, D. A., "Release Rates for Xenon and Cesium from Moderate and High Burnup Reactor Fuel," Issued as a Technical Note, September, 2013.
3. "Impact of High Burnup Uranium Oxide and Mixed Uranium-Plutonium Oxide Water Reactor Fuel on Spent Fuel Management," IAEA Nuclear Energy Series No. NF-T-3.8.
4. "Observations on the release of cesium from UO_2 fuel," C.T. Walker, C. Bagger, M. Mogensen, Journal of Nuclear Materials 240 (1996) 32-42.

Comment #7: DG 1327, Appendix B, Section B-2.1.1.

Statement in Guidance: Equations shown below.

$$\left(\frac{R}{B}\right)_{i,m} = \left(\frac{S}{V}\right)_{i,m}\sqrt{\frac{\alpha_{nuclide}D_{i,m}}{\lambda_{nuclide}}}$$

$$\left(\frac{R}{B}\right)_{i,nuclide} = F_{nuclide}\left(\frac{S}{V}\right)_{i}\sqrt{\frac{\alpha_{Kr-85m}D_{i}}{\lambda_{Kr-85m}}}$$

Description of Concern: To facilitate understanding, a definition of the terms used in the above equations should be provided.

Basis for concern: Clarity.

Proposal: Provide definition of terms from Reference 1 for clarity and completeness.

Basis for Proposal: Clarity.

References:

1. "Background and Derivation of ANS-5.4 Standard Fission Product Release Model," NUREG/CR-7003 (PNNL-18490), January 2010.